Asymptotic scaling in Hamiltonian calculations of the O(3) σ model

Anthony Duncan and Ralph Roskies
Department of Physics, University of Pittsburgh, Pittsburgh, Pennsylvania 15260
(Received 9 May 1985)

By extending Hamiltonian variational techniques of a previous paper, we are able to calculate mass gaps in the asymptotic scaling region of the O(3) σ model.

I. INTRODUCTION

Reliable techniques for extracting the mass spectrum of asymptotically free theories in the scaling region are crucial for testing the validity of QCD at low energies. So far, the attack on this problem largely has been via Monte Carlo simulations. Even in pure Yang-Mills SU(3) simulations for the β function in $3+1$ dimensions, the region of asymptotic scaling (the one- or two-loop regime) has not been reached.[1]

In this paper, we report on an extension of a variational technique (introduced in a previous paper[2] to be referred to as I) which allows us to get reliable mass estimates in the one-loop scaling region for the O(3) σ model in $1+1$ dimensions. As far as we know, no other techniques have allowed reliable penetration of that deep scaling regime.

Our technique, based on the Hamiltonian formulation, chooses as a trial wave function an optimal linear combination of states occurring in $H^n|\psi_0\rangle$, where H is the Hamiltonian and $|\psi_0\rangle$ an original trial wave function. We extend the results of I by going to one more order in H, on a sufficiently large lattice. (We require much smaller lattices than in comparable Monte Carlo calculations.) Our results are in excellent agreement with continuum scaling formulas. We also discuss the results in the context of the finite-size scaling arguments of Fisher[3] and Brézin.[4]

As a byproduct, we obtain approximate wave functions for the ground state and first excited state. Although it is unlikely that these approximate wave functions reliably capture all details of the true wave functions, they are close enough to give reliable energy estimates. We intend to investigate features of the wave function in a later work.

In the next section, we briefly review the techniques of I and indicate how they are extended. Our results are presented in Sec. III. In Sec. IV, we discuss finite-size scaling effects. Section V contains brief conclusions.

II. GENERAL THEORY

Our Hamiltonian is

$$H=\frac{1}{a}\left[\beta\sum_n L_n^2+\frac{1}{2\beta}\sum_n(1-\boldsymbol{\phi}_n\cdot\boldsymbol{\phi}_{n+1})\right], \tag{2.1}$$

where the sum is over the one-dimensional spatial lattice sites, $\boldsymbol{\phi}_j$ is a unit vector at lattice site j, a is the lattice spacing, and

$$L_n^2=\boldsymbol{\phi}_n\cdot\frac{\partial}{\partial\boldsymbol{\phi}_n}\left[\boldsymbol{\phi}_n\cdot\frac{\partial}{\partial\boldsymbol{\phi}_n}+1\right]+\boldsymbol{\phi}_n\cdot\boldsymbol{\phi}_n\frac{\partial}{\partial\boldsymbol{\phi}_n}\cdot\frac{\partial}{\partial\boldsymbol{\phi}_n}. \tag{2.2}$$

Small β is the weak-coupling regime. The lattice is introduced to regulate the divergences of the continuum theory. We choose free boundary conditions $\boldsymbol{\phi}_0=\boldsymbol{\phi}_{L+1}=0$ where L is the number of lattice sites.

In I the original trial function in the scalar sector was

$$|\psi_s\rangle=\exp\left[\lambda\sum_n\boldsymbol{\phi}_n\cdot\boldsymbol{\phi}_{n+1}\right]|0\rangle, \tag{2.3}$$

where $|0\rangle$ is the strong-coupling vacuum defined by

$$L_j^2|0\rangle=0 \quad \text{for all } j. \tag{2.4}$$

We had found that

$$H|\psi_s\rangle \tag{2.5}$$

contained a linear combination of four additional topologically distinct states, providing a five-dimensional basis for minimizing the ground-state energy.

Similarly, in the triplet sector, our starting point was

$$|\psi_{t,\alpha}\rangle=\left[\sum_j\phi_j^\alpha\right]\exp\left[\lambda\sum_n\boldsymbol{\phi}_n\cdot\boldsymbol{\phi}_{n+1}\right]|0\rangle, \tag{2.6}$$

where α is an isospin index. $H|\psi_{t,\alpha}\rangle$ contained a linear combination of six additional states.

In this paper, we extend our results to the basis states contained in $H^2|\psi_s\rangle$ and $H^2|\psi_t\rangle$ which are 26 and 60 dimensional, respectively. (The singlet basis states are listed in the Appendix.) The calculation consists of diagonalizing the Hamiltonian H in the 26- and 60-dimensional subspaces, respectively, and interpreting the lowest eigenvalues as (over) estimates for the energies of the ground state and zero-momentum first excited states, respectively. The mass gap is the difference between these two energies.

As explained in I, this is a completely analytic calculation, but the matrix elements of the Hamiltonian H are such complicated functions of λ that they are evaluated by a FORTRAN program, based on formulas produced by a REDUCE program. The numerical evaluation is by far the most time consuming. For example, for each value of λ, the 26×26 matrix evaluated on a 16-site lattice required 45 min on a RIDGE-32, while the 60×60 matrix required 20 h. Each of these were evaluated at several values of λ,

TABLE I. Lowest-lying energies in the singlet and triplet sectors on a lattice of size $L=8$ as a function of coupling. These are minimized in spaces of dimension 5 and 26 for the singlet and dimension 7 and 60 for the triplet. The mass gap is the difference between triplet and singlet energies.

	Singlet		Triplet			
	5-dimensional	26-dimensional	7-dimensional	60-dimensional	Mass gap	
β	basis	basis	basis	basis	7—5	60—26
0.30	7.449	7.403	7.541	7.515	0.091	0.112
0.31	7.374	7.332	7.480	7.456	0.106	0.123
0.32	7.298	7.260	7.419	7.396	0.121	0.135
0.33	7.221	7.187	7.358	7.335	0.136	0.148
0.34	7.144	7.113	7.297	7.275	0.153	0.162
0.35	7.065	7.038	7.236	7.215	0.172	0.177

and the final estimate for the energies was obtained by searching for the minimum in λ by quadratic interpolation. Some details of the REDUCE calculations will be published elsewhere.[5]

III. RESULTS

In Tables I, II and III we present results for lattices of size 8, 12, and 16 indicating for each value of β in the weak-coupling regime the energy estimate based on the basis generated by $H|\psi\rangle$ and by $H^2|\psi\rangle$. One can see immediately that for the larger lattices, for weak coupling, the small mass gap is the difference between two large numbers, which must therefore be evaluated quite precisely. (It is not even guaranteed that the mass gap turn out positive.)

It should be emphasized that we are in the region of mass gaps very small compared to an inverse lattice spacing, so that we can hope for a good approximation of continuum results. However, we expect infrared effects, especially for the small lattices, to be present.

Several general features can be observed from the results. The increased basis reduces the singlet energy estimate more than the triplet estimate, thereby increasing the mass gap. At larger values of β, this effect is smaller so that the smaller basis already gives a good estimate of the mass gap. At small β, the increased basis is essential. We believe that at the very smallest value $\beta=0.30$, even the 26- and 60-dimensional bases do not quite suffice to accurately describe the mass gap.

We can compare our results to the continuum scaling behavior. The $(1+1)$-dimensional σ model is an asymptotically free theory, and to three loops, the relation between the lattice spacing and coupling β is[6]

$$a=\frac{1}{\Lambda}\exp\left[-\frac{1}{t}-\ln t-\frac{t}{4}\right],\quad t=\beta/\pi\ . \tag{3.1}$$

Defining $m_\infty(\beta)$ to be the expected mass gap in the continuum[7]

$$am_\infty(\beta)=(101)\exp\left[-\frac{1}{t}-\ln t-\frac{t}{4}\right] \tag{3.2}$$

we plot, in Fig. 1, $m(\beta)/m_\infty(\beta)$ versus β where $m(\beta)$ is the observed mass gap. If $m(\beta)$ scaled, the graph would be flat. Note that although β ranges only between 0.30 and 0.35, $m_\infty(\beta)$ falls by a factor of more than 3 in this regime. It is clear that the $O(H^2)$ results for $L=16$ show excellent agreement with scaling. This confirms the presence of infrared effects for small lattices, and the need for large bases in the weak-coupling region for large lattices.

In Fig. 2, we present the results somewhat differently. We plot $\ln m(\beta)$ versus $1/\beta$. If one-loop scaling were correct, this should be a straight line of slope $-\pi$. Such a line is shown on the plot, and gives a good approximation to the best straight line through the observed data points.

TABLE II. Lowest-lying energies in the singlet and triplet sectors on a lattice of size $L=12$ as a function of coupling. These are minimized in spaces of dimension 5 and 26 for the singlet and dimension 7 and 60 for the triplet. The mass gap is the difference between triplet and singlet energies.

	Singlet		Triplet			
	5-dimensional	26-dimensional	7-dimensional	60-dimensional	Mass gap	
β	basis	basis	basis	basis	7—5	60—26
0.30	11.706	11.618	11.742	11.680	0.036	0.061
0.31	11.587	11.507	11.639	11.581	0.053	0.074
0.32	11.467	11.395	11.536	11.482	0.069	0.087
0.33	11.345	11.281	11.433	11.382	0.088	0.101
0.34	11.223	11.165	11.330	11.282	0.107	0.116
0.35	11.099	11.048	11.226	11.181	0.126	0.133

TABLE III. Lowest-lying energies in the singlet and triplet sectors on a lattice of size $L=16$ as a function of coupling. These are minimized in spaces of dimension 5 and 26 for the singlet and dimension 7 and 60 for the triplet. The mass gap is the difference between triplet and singlet energies.

	Singlet		Triplet			
	5-dimensional	26-dimensional	7-dimensional	60-dimensional	Mass gap	
β	basis	basis	basis	basis	7—5	60—26
0.30	15.9709	15.8414	15.9752	15.8710	0.0043	0.0296
0.31	15.8075	15.6895	15.8307	15.7334	0.0232	0.0439
0.32	15.6424	15.5355	15.6839	15.5942	0.0415	0.0587
0.33	15.4756	15.3795	15.5373	15.4542	0.0617	0.0747
0.34	15.3072	15.2214	15.3892	15.3129	0.0820	0.0915
0.35	15.1378	15.0616	15.2407	15.1707	0.1029	0.1091

IV. FINITE-SIZE SCALING

The results presented above may be organized in a somewhat different fashion, to exhibit more directly the influence of finite-size effects on the mass gap. Only if those effects are small— or controllable—can we expect our results to be relevant to the continuum field theory being modeled. The finite-size scaling theory, introduced by Fisher,[3] and applied to the N-vector model for large N by Brézin,[4] suggests the appropriate reparametrization of the mass-gap results. In the limit of large L, $\beta\to\beta_c$ (where β_c represents a critical point of diverging correlation lengths for the *infinite-size* system), finite-size scaling asserts

$$\frac{m_L(\beta)}{m_\infty(\beta)}=f(Lm_\infty(\beta))\equiv f(x)\ , \tag{4.1}$$

where $m_L(\beta)$ is the mass gap on a lattice of L sites, and f is a universal function. By taking the limit $L\to\infty$ (fixed β) in (4.1), it is manifest that $f(x)\to 1$ for large x. However, the regions of small and large x are *both* inaccessible in approximate calculations of the mass gap, for the following reasons.

(a) For small x, the necessity for having L large in (4.1) forces us to very small values for $m_\infty(\beta)$, i.e., in the deep weak-coupling regime where both variational and Monte Carlo calculations will encounter difficulties. In our approach, for example, if $g(\beta)\to 0$ at fixed L, the vacuum sector energy is eventually overestimated (relative to the one-particle sector) to the point of driving the mass gap negative. In other words, accurate calculation of $m_L(\beta)$ in this region would require the use of large bases. Of

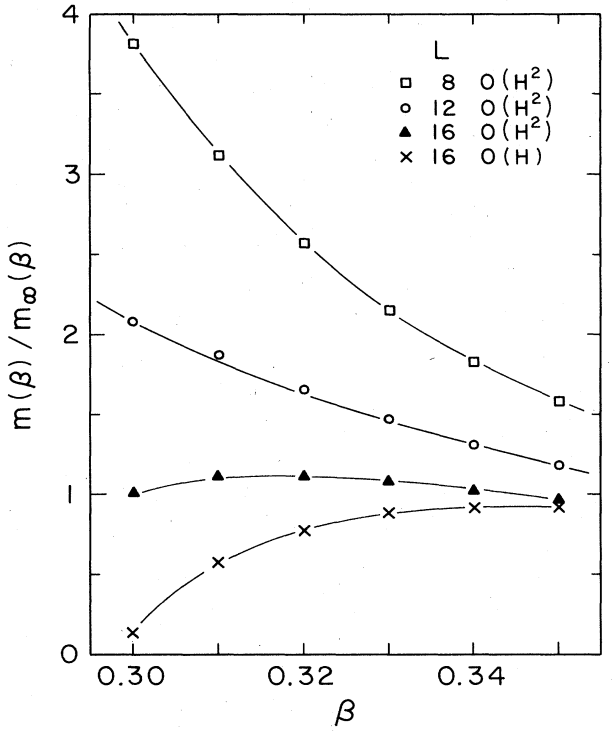

FIG. 1. Plot of the ratio (calculated mass gap)/(three-loop continuum formula for the mass gap) vs coupling on lattices of size 8, 12, and 16, in bases of 26 and 60 dimensions for the singlet and triplet. For a 16-lattice, the results for the smaller bases (5 and 7 dimensions) are also given. Asymptotic scaling implies that the ratio should be flat.

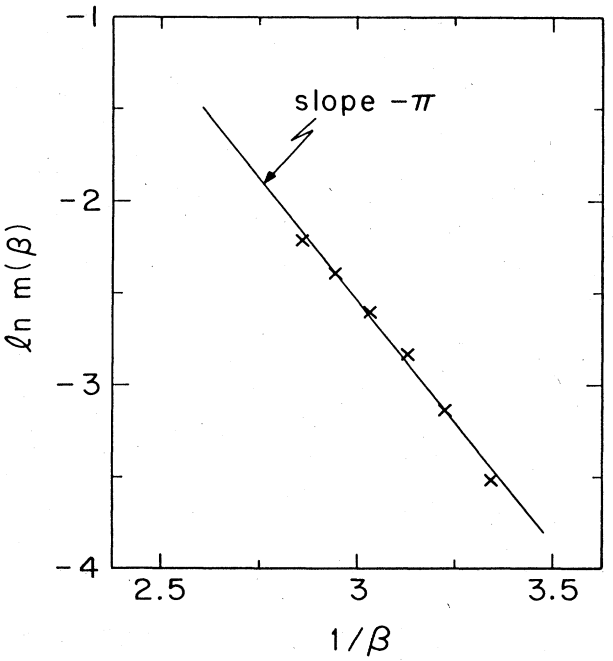

FIG. 2. Plot of mass gap vs coupling for a 16-lattice using bases of size 26 and 60. The solid line is the one-loop scaling result.

course, this is precisely the region in which $m_\infty(\beta)$ is controlled by the renormalization group.

(b) For large x, fixed L, we are eventually forced out of the critical region $m_\infty(\beta) \ll 1$. This problem is especially severe for the O(3) mass gap, as perturbative scaling does not set in until one reaches mass gaps ~ 0.05. In order to study this region accurately, therefore, one would be forced to very large lattices.

It is apparent that approximate methods (whether variational or Monte Carlo) will only determine f in an intermediate region—yet another example of the "asymptotic freedom window" frequently discussed by lattice practitioners.

Our results are shown in Fig. 3, where we plot $f(x)$ for $0.5 < x < 3.5$, for lattice sizes $L = 8,12,16$. For $x > 1.7$, the values computed with any of these lattices fall below 1, indicating a departure from the critical region $[m_\infty(\beta) > m_L(\beta)$ in the strong- and intermediate-coupling regime]. The results for the smaller lattices $L = 8,12$ show no flattening around $f = 1$, but for $L = 16$ there is a flattening in the intermediate region $0.6 < x < 0.9$. This "window" corresponds precisely to the region of scaling discussed previously. The evidence suggests that we do not see finite-size scaling for $L < 16$. As pointed out previously, below $x \sim 0.6$ for $L = 16$ we lose convergence in the variational scheme. For $x > 2$, the values obtained for all three lattices agree tolerably (the mass gap is simply not very sensitive to the size of the lattice in this region), but nonperturbative contributions to scaling result in a considerable deviation from the ideal scaling limit $f \to 1$.

It should be noted that we have used free boundary conditions and it may well be the case that finite-size scaling is adversely affected on smaller lattices by such a choice.

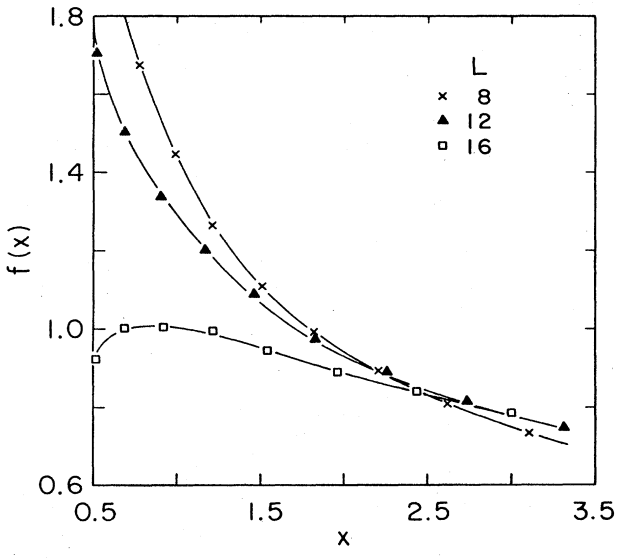

FIG. 3. Plot of $f(x)$=(observed mass gap)/(three-loop continuum formula for mass gap) on lattices of size 8, 12, and 16 vs $x = Lm_\infty(\beta)$, where L is the lattice size and $m_\infty(\beta)$ is the continuum three-loop formula for the mass gap. Finite-size scaling predicts a universal curve.

Another feature which complicates finite-size scaling in the O(3) model is the logarithmic scaling at the critical point—models with power scaling at criticality (e.g., Ising models) appear to give a universal $f(x)$ over substantial regions of x even for quite small lattices.[8]

V. CONCLUSIONS

The results of Sec. III, especially those in Fig. 1, show excellent agreement with asymptotic scaling predictions. They emphasize that large lattices are needed for small masses (large correlation lengths), and that large enough bases for the variational estimates are required to really see the scaling behavior. The remarkable finding is that the computation of expectation values of the Hamiltonian appears to be accurate down to mass gaps on the order of $0.05/a$ even though the wave functions involved contain structures with direct coupling between spins separated at most by $3a$. We conjecture that this will be true for other local operators, but very likely not for bilocal (see below) or multilocal operators.

In other words, computation of $\langle \psi_{gs} | H | \psi_{gs} \rangle$ seems much less sensitive to the detailed structure of the state than a naive estimate in terms of the explicit spin-spin correlation structure of $|\psi_{gs}\rangle$ would indicate. We also realized in I that for fixed basis size, going to very large lattices can give poor results because the overlap of the approximate wave function and the true one gets worse and worse. It is crucial to understand the interplay between basis size and lattice size, especially for weak coupling.

As emphasized in the Introduction, the variational method allows us to find the ground-state wave function as well as the ground-state energy. From this, we could in principle compute many other physical properties. For example, we could estimate the mass gap by looking for the exponential falloff of the expectation value of

$$\langle \psi_{gs} | \boldsymbol{\phi}_i \cdot \boldsymbol{\phi}_{i+\kappa} | \psi_{gs} \rangle$$

with κ for some fixed i. We intend to compute this quantity, but expect it to give a worse estimate of the mass gap than our direct Hamiltonian approach. (In particular, it is likely that the correlation length estimated by this procedure does correspond roughly to the most extended structure in the wave function.)

One could also estimate the mass gap if the lowest excited state in the scalar sector were formed by two triplets, sufficiently far that they would not interact. Then the lowest excitation energy in the scalar sector would be $2m$, where m is the mass gap. Our results have not yet yielded any stable estimate for this excitation energy. It is still too large, keeps decreasing as we increase the basis, and does not scale appropriately. One reason is that $2m$ is the onset of a branch point, rather than a pole, in the propagator, and the excited state value we obtain numerically is the effect of the whole cut, most of whose contribution comes at a higher energy than $2m$.

We are sufficiently encouraged by our results for the $(1+1)$-dimensional σ model, that we are now beginning a study of the spectrum of $(3+1)$-dimensional SU(3) Yang-Mills theory.

ACKNOWLEDGMENTS

This work was supported in part by the National Science Foundation, Washington, D.C. A.D. wishes to acknowledge the support of the Alfred P. Sloan Foundation, and R.R. would like to thank Harvard University for its hospitality during his sabbatical.

APPENDIX

To illustrate the type of structures encountered, we list the 26-dimensional basis used in the scalar sector.

Let

$$|\lambda\rangle = \exp\left[\lambda \sum_i \boldsymbol{\phi}_i \cdot \boldsymbol{\phi}_{i+1}\right] |0\rangle , \tag{A1}$$

where $|0\rangle$ is the strong-coupling vacuum. Then our basis states are

$$\begin{aligned}
|1\rangle &= |\lambda\rangle , \\
|2\rangle &= \sum \boldsymbol{\phi}_i \cdot \boldsymbol{\phi}_{i+1} |\lambda\rangle , \\
|3\rangle &= \sum (\boldsymbol{\phi}_i \cdot \boldsymbol{\phi}_{i+1})^2 |\lambda\rangle , \\
|4\rangle &= \sum \boldsymbol{\phi}_i \cdot \boldsymbol{\phi}_{i+1} \boldsymbol{\phi}_{i+1} \cdot \boldsymbol{\phi}_{i+2} |\lambda\rangle , \\
|5\rangle &= \sum \boldsymbol{\phi}_i \cdot \boldsymbol{\phi}_{i+2} |\lambda\rangle , \\
|6\rangle &= \sum (\boldsymbol{\phi}_i \cdot \boldsymbol{\phi}_{i+1})^3 |\lambda\rangle , \\
|7\rangle &= \sum (\boldsymbol{\phi}_i \cdot \boldsymbol{\phi}_{i+1})(\boldsymbol{\phi}_{i+1} \cdot \boldsymbol{\phi}_{i+2})^2 |\lambda\rangle , \\
|8\rangle &= \sum (\boldsymbol{\phi}_i \cdot \boldsymbol{\phi}_{i+1})^2 (\boldsymbol{\phi}_{i+1} \cdot \boldsymbol{\phi}_{i+2}) |\lambda\rangle , \\
|9\rangle &= \sum \boldsymbol{\phi}_i \cdot \boldsymbol{\phi}_{i+1} \boldsymbol{\phi}_i \cdot \boldsymbol{\phi}_{i+2} |\lambda\rangle , \\
|10\rangle &= \sum \boldsymbol{\phi}_i \cdot \boldsymbol{\phi}_{i+2} \boldsymbol{\phi}_{i+1} \cdot \boldsymbol{\phi}_{i+2} |\lambda\rangle , \\
|11\rangle &= \sum \boldsymbol{\phi}_i \cdot \boldsymbol{\phi}_{i+3} |\lambda\rangle , \\
|12\rangle &= \sum \boldsymbol{\phi}_i \cdot \boldsymbol{\phi}_{i+2} \boldsymbol{\phi}_{i+2} \cdot \boldsymbol{\phi}_{i+3} |\lambda\rangle ,
\end{aligned} \tag{A2}$$

$$\begin{aligned}
|13\rangle &= \sum \boldsymbol{\phi}_i \cdot \boldsymbol{\phi}_{i+1} \boldsymbol{\phi}_{i+1} \cdot \boldsymbol{\phi}_{i+3} |\lambda\rangle , \\
|14\rangle &= \sum \boldsymbol{\phi}_i \cdot \boldsymbol{\phi}_{i+1} \boldsymbol{\phi}_{i+1} \cdot \boldsymbol{\phi}_{i+2} \boldsymbol{\phi}_{i+2} \cdot \boldsymbol{\phi}_{i+3} |\lambda\rangle , \\
|15\rangle &= \sum \boldsymbol{\phi}_i^2 \boldsymbol{\phi}_{i+1} \cdot \boldsymbol{\phi}_{i+2} |\lambda\rangle , \\
|16\rangle &= \sum \boldsymbol{\phi}_i \cdot \boldsymbol{\phi}_{i+1} \boldsymbol{\phi}_{i+2}^2 |\lambda\rangle , \\
|17\rangle &= \left[\sum \boldsymbol{\phi}_i \cdot \boldsymbol{\phi}_{i+1}\right]^2 |\lambda\rangle , \\
|18\rangle &= \left[\sum \boldsymbol{\phi}_i \cdot \boldsymbol{\phi}_{i+1}\right] \left[\sum (\boldsymbol{\phi}_j \cdot \boldsymbol{\phi}_{j+1})^2\right] |\lambda\rangle , \\
|19\rangle &= \left[\sum \boldsymbol{\phi}_i \cdot \boldsymbol{\phi}_{i+1}\right] \left[\sum \boldsymbol{\phi}_j \cdot \boldsymbol{\phi}_{j+1} \boldsymbol{\phi}_{j+1} \cdot \boldsymbol{\phi}_{j+2}\right] |\lambda\rangle ,
\end{aligned} \tag{A3}$$

$$\begin{aligned}
|20\rangle &= \left[\sum \boldsymbol{\phi}_i \cdot \boldsymbol{\phi}_{i+1}\right] \left[\sum \boldsymbol{\phi}_j \cdot \boldsymbol{\phi}_{j+2}\right] |\lambda\rangle , \\
|21\rangle &= \left[\sum (\boldsymbol{\phi}_i \cdot \boldsymbol{\phi}_{i+1})^2\right]^2 |\lambda\rangle , \\
|22\rangle &= \left[\sum (\boldsymbol{\phi}_i \cdot \boldsymbol{\phi}_{i+1})^2\right] \left[\sum \boldsymbol{\phi}_j \cdot \boldsymbol{\phi}_{j+1} \boldsymbol{\phi}_{j+1} \cdot \boldsymbol{\phi}_{j+2}\right] |\lambda\rangle , \\
|23\rangle &= \left[\sum (\boldsymbol{\phi}_i \cdot \boldsymbol{\phi}_{i+1})^2\right] \left[\sum \boldsymbol{\phi}_j \cdot \boldsymbol{\phi}_{j+2}\right] |\lambda\rangle , \\
|24\rangle &= \left[\sum \boldsymbol{\phi}_i \cdot \boldsymbol{\phi}_{i+1} \boldsymbol{\phi}_{i+1} \cdot \boldsymbol{\phi}_{i+2}\right]^2 |\lambda\rangle , \\
|25\rangle &= \left[\sum \boldsymbol{\phi}_i \cdot \boldsymbol{\phi}_{i+1} \boldsymbol{\phi}_{i+1} \cdot \boldsymbol{\phi}_{i+2}\right] \left[\sum \boldsymbol{\phi}_j \cdot \boldsymbol{\phi}_{j+2}\right] |\lambda\rangle , \\
|26\rangle &= \left[\sum \boldsymbol{\phi}_i \cdot \boldsymbol{\phi}_{i+2}\right]^2 |\lambda\rangle .
\end{aligned} \tag{A4}$$

The first five states occur in $H|\lambda\rangle$, the rest in $H^2|\lambda\rangle$. We see that the connected structures extend over at most three lattice sites. These are all translationally invariant states, but we have used free boundary conditions $\boldsymbol{\phi}_j = 0$ if $j < 1$ or $j > N$. Thus $|16\rangle$ is obtained from $|2\rangle$ by omitting the term $i = N-1$ in the sum occurring in $|2\rangle$.

[1]See, e.g., *Proceedings of the Lattice Gauge Theory Conference 1985,* edited by Dennis Duke (Florida State University, Tallahassee, 1985).

[2]A. Duncan and R. Roskies, Phys. Rev. D **31**, 364 (1985).

[3]M. E. Fisher, in *Critical Phenomena,* proceedings of the 51st Enrico Fermi Summer School, Varenna, edited by M. S. Green (Academic, New York, 1972); M. E. Fisher and M. N. Barber, Phys. Rev. Lett. **28**, 1516 (1972).

[4]E. Brezin, J. Phys. (Paris) **43**, 15 (1982).

[5]A. Duncan and R. Roskies, J. Symbol. Comput. (to be published).

[6]S. Hikami and E. Brezin, J. Phys. A **11**, 1141 (1978).

[7]The constant 101 is a rough estimate chosen to make $m(\beta)$ comparable to $m_\infty(\beta)$. It is consistent with the estimates of H. Arisue, Phys. Lett. **140B**, 383 (1984); M. Fukugita and Y. Oganagi, *ibid.* **123B**, 71 (1983); and the strong-coupling result of J. Shigemitsu and J. B. Kogut, Nucl. Phys. **B190** [FS3], 365 (1981).

[8]J. Zinn-Justin (private communication).